A COST BASED APPROACH TO DESIGN OF RESIDENTIAL STEEL ROOF SYSTEMS

B. Mobasher[1], S-Y.Chen[2], C. Young[2] and S. D. Rajan[3]
Department of Civil Engineering
Arizona State University
Tempe, AZ 85287-5306

Abstract

A comprehensive system for the design of residential steel roof truss systems is presented. The research involved three distinct stages. In the first stage, components of the truss systems were tested in order to determine their member properties subjected to axial force and bending moments. Finite element simulations of these tests were carried out to further verify the calculations obtained using the AISI-LRFD code guidelines. The AISI-LRFD code based design curves were used for the actual design, the laboratory experiments and the finite element results provided additional checks and verification of the AISI values. The second stage of the research involved the development of an integrated design system that would automatically design a roof truss given minimal input and using the design curves as the performance constraints. A design optimization scheme based on the genetic algorithm was adopted to handle sizing, shape and topology variables in the design problem. A software system was developed to design the lowest cost truss given the input parameters. The third stage of the research involved full-scale testing of typical residential steel roofs designed using the developed software system. Roof trusses were loaded to failure. The full scale testing procedure established the factor of safety while validating the analysis and design procedures. Evaluation of the test results indicates that the present design system provides enough reserve strength for the structure to perform as predicted.

1.0 Introduction

Steel is one of the primary materials for structural systems. However, it is only recently that its use for residential buildings is being explored. The focus of the current research is on three aspects of increasing the application of steel products in residential and commercial construction markets. The first deals with the use of steel sections as the primary load bearing members. Experimental techniques are used to evaluate the load-carrying capacity of the individual cross-sections and to establish the guidelines for connections. This will lead to the generation of design criteria for the members and connections. The second focus area is directed toward development of a system based approach in the design methodologies for optimum use of steel members as a system. The last focus area is on the validation of the developed analysis and design procedures using full-scale testing.

---

[1] Associate Professor. Member ASCE
[2] Graduate Assistant
[3] Professor. Member ASCE, ASME.

The load and resistance factor design (LRFD) criteria have been developed for both hot-rolled (AISC: Load and Resistance Factor Design, 1986) and cold-formed steel sections. (Hsiao, Yu and Galambos, 1990). Guidelines for the AISI-LRFD design of cold-formed members are used in the present approach. The paper is organized into several sections. The first part discusses the development of the design curves. This is followed by a discussion of the optimal design methodology used in designing the lowest cost truss. Results from a specific example are discussed. This specific design is then used in the full-scale test that is discussed in the final part of the paper.

In the present work, roof truss systems are constructed using two different cross-section types - open and closed channel sections of various thickness as manufactured by Allied American Inc., Phoenix, Arizona. Fig. 1(a) shows the typical (open) chord cross section. The design domain is constructed with open channel sections that are 2.5" and 3.5" deep, in three different thickness or gauges - 16 GA., 18 GA. and 20 GA. Similarly, a typical (closed) web member is shown in Fig. 1(b). Mechanical tests were conducted to evaluate the performance of the individual members, fasteners, and connectors. Three different loading conditions of compression, flexure, and tension were used. The experimentally obtained failure loads were compared to the values from the AISI code as well as from finite element analysis. Using the basic test results, the design curves are developed. These curves are then used in an automated design process to check the adequacy of each design while finding the truss with the lowest cost. To validate the design process and methodology, a full-scale test was conducted for the truss design with the lowest cost.

2.0 Design Curves

In order to design the different truss members, it is necessary to construct the design curves that indicate the allowable internal stresses in any member. For the open section members, this task is achieved in three different ways. First, mechanical testing is carried out on individual members. Second, a finite element simulation (of the test procedure) is conducted. Finally, the AISI-LRFD code is used to compute the same values. The motivation is to ensure that the AISI code based values are applicable with adequate factor of safety to the cross-sections used.

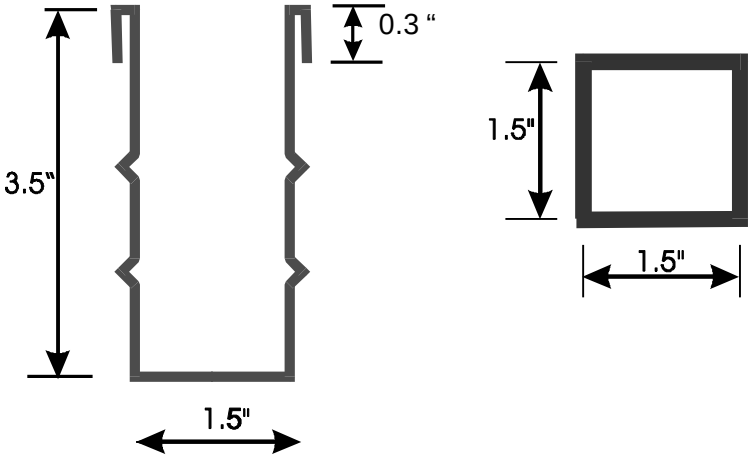

Fig. 1 (a) Typical chord section (designation: *3.5 CHORD 16GA, also available as 2.5" deep section and gages 18 and 20)* (b) square section for web and heel section (designation: *1.5 SQWEB 16GA, also available in 18 and 20 gages*

2.1 Mechanical Tests

Experimental work was conducted by Weng and Pekoz [1990] to characterize the compression tests of cold-formed steel columns. In the present study, tests were performed on a closed-loop servohydraulic test machine under displacement control. The capacity of the loading frame was 220 kN (55 kips). Tests were controlled using the TestStar software package developed by MTS Corp (Minn, MN).

2.1.1 Axial Compression Tests

The compressive response (from four replicate samples of four different lengths) for each of the various sections were determined. The displacement rate of the actuator was used as the control parameter. The specimen ends were attached to the load frame by means of a rigid connection. A constant displacement rate was applied to the end plate while the load was measured using a load cell. Since the test was conducted under constant displacement, the failure of the specimen was gradual. As the large deformations accumulate due to global or localized buckling, the servo-loop control system reduced the load so that the rate of displacement is maintained equal to the prescribed level. The test was terminated well beyond the ultimate load carrying capacity. This displacement level was chosen as 0.5" for the 18 and 20 GA. specimens, and 0.6" for the 16 GA. specimens.

Fig. 3 shows a typical load-displacement response in compression for various length specimens of 18 gage. The test is terminated in the post peak region of the response when the vertical displacement exceeds the prescribed value. Figure 4 shows the (mean) ultimate load obtained for the different chord specimens. Note that as the length of the section increases the axial capacity decreases. In addition the scatter in the data increases as the length decreases and local buckling dominates the failure.

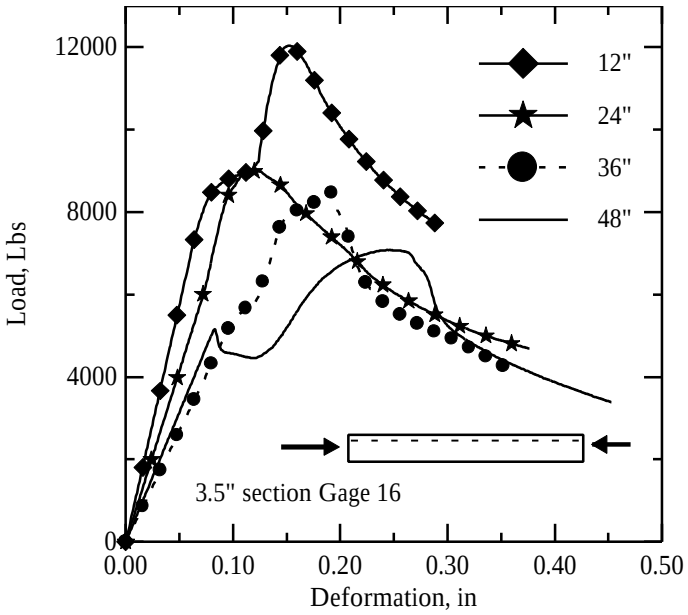

Fig. 3 Load-displacement curve for 2.5 Chord18GA 12"-48" specimens axial compression test

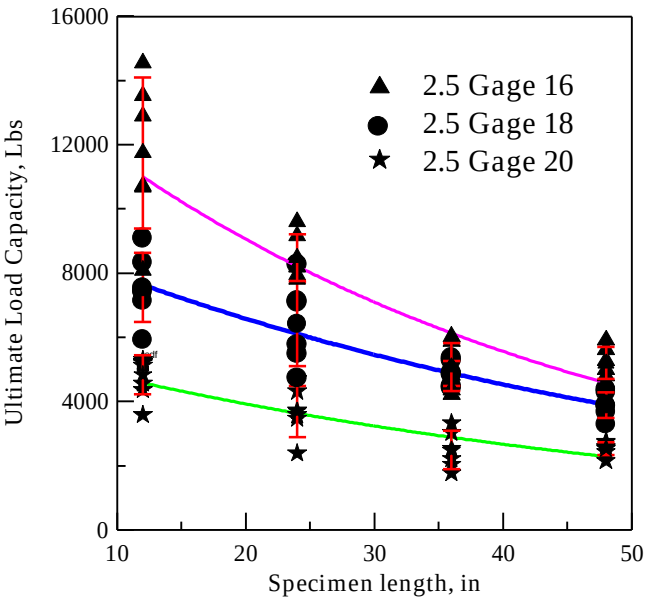

Fig. 4 Experimentally obtained ultimate load (mean value) for the different specimens

2.1.2 Flexural Tests

Flexural response of various sections were determined using a four point bending test (Fig. 5). The objective of this test was to compute the maximum bending moment that the sections can withstand under braced conditions. The plastic moment capacity was of primary importance at this stage of testing; hence the torsional buckling was neglected in the flexural mode. Specimens were simply supported on the loading fixture. A constant span of 24" was used for all the specimens. Two line loads spaced at 4.75" apart were used to apply the flexural forces. In order to prevent local crushing of the specimen due to stress concentration, steel plates 1/4" in thickness were used under the loading points. Specimen deflections were measured using a Linear Variable Differential Transformer (LVDT). Tests were terminated at a vertical displacement of 0.8" for negative moment and 0.4" for positive moments. Two replicate tests per section were conducted for each positive and negative bending moment tests. Positive moment was defined as causing compression in the flange, where as negative moment caused tension in the flange.

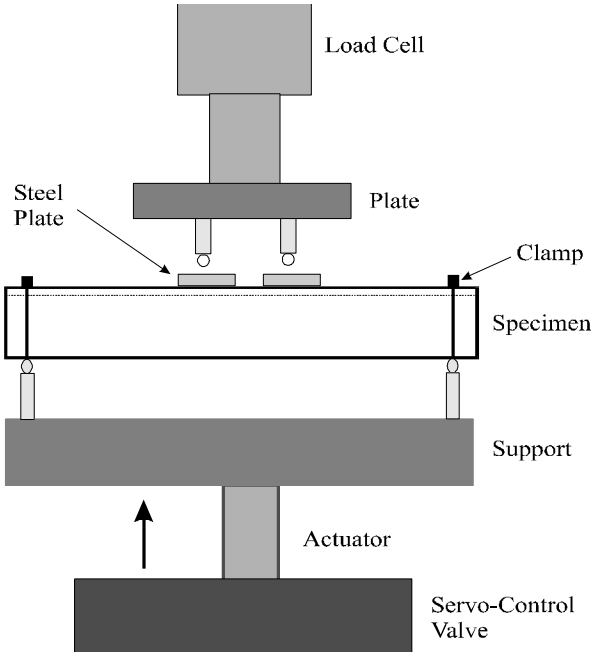

Fig. 5 Test setup for the four-point bending test

2.2 Finite Element Simulations

As an alternate approach to verify the test results and the AISI guidelines, the finite element method was used to compute the strength of the members. An eigenvalue problem was formulated using a linearized buckling analysis procedure. Further details can be obtained in [Wright et. al., 1995]. Fig. 6 shows the first mode of buckling obtained from the linearized buckling analysis. In addition to Euler type buckling, finite element method was also used to study the local buckling phenomenon in the sections. Schematics of this mode of failure are shown in figure 6.b.

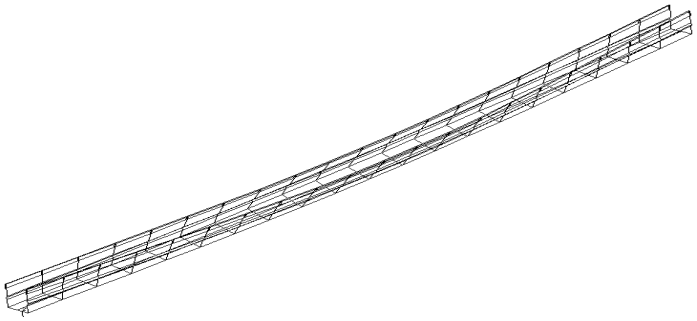

Fig. 6a The first mode of buckling obtained from a linear finite element simulation for axial compression test

Fig. 6b The local buckling mode of buckling obtained from a linear finite element simulation for flexural loading.

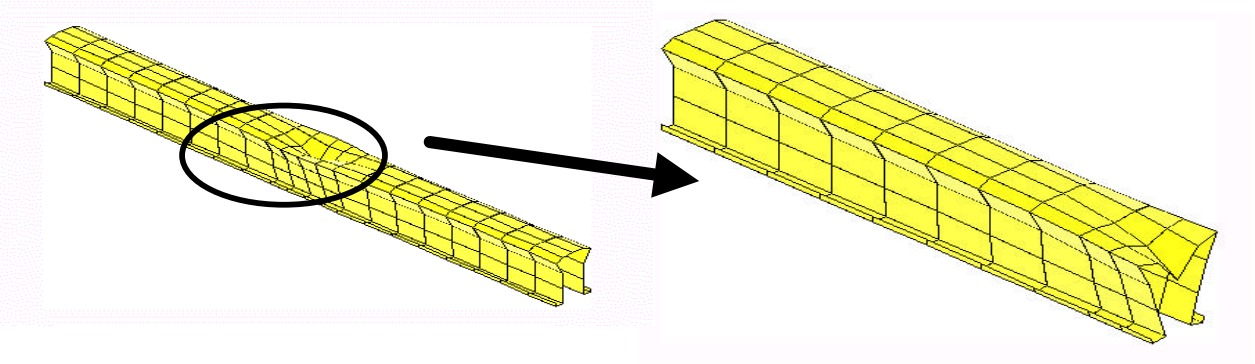

2.3 AISI-LRFD Calculations

Finally, the AISI-LRFD design code was used to compute the corresponding values of the different cross-sections. The details of the code provisions and the relevant calculations are not shown here. They are however available in a research report [Mobasher and Situ, 1996]. The values for the *Axial Compression* obtained from the laboratory, AISI-LRFD design code and finite element analysis are compared in Table 1.

		Ultimate Load (lb)					
		3.5 CHORD			2.5 CHORD		
Length	Source	20 GA	18 GA	16 GA	20 GA	18 GA	16 GA
12 "	AISI-LRFD	3176	4376	7035	3224	4447	7176
	FEA	3290	5359	8432	3623	6256	9726
	Exp. Mean	4900	9643	11488	4576	6979	11296
24"	AISI-LRFD	2729	3729	5788	3071	4200	6706
	FEA	2353	3932	6371	2896	4814	8061
	Exp. Mean	4852	8039	9593	4052	7065	8696
36"	AISI-LRFD	1882	2624	3776	2788	3800	5918
	FEA	2007	3554	5874	2712	4528	6635
	Exp. Mean	4203	6953	7785	2727	5090	5342
48"	AISI-LRFD	1259	1765	2576	2353	3224	4835
	FEA	1908	3396	5415	2313	3252	4505
	Exp. Mean	3324	3755	8143	2477	4049	5279

Table 1 Comparison of Results for the Axial Compression Test

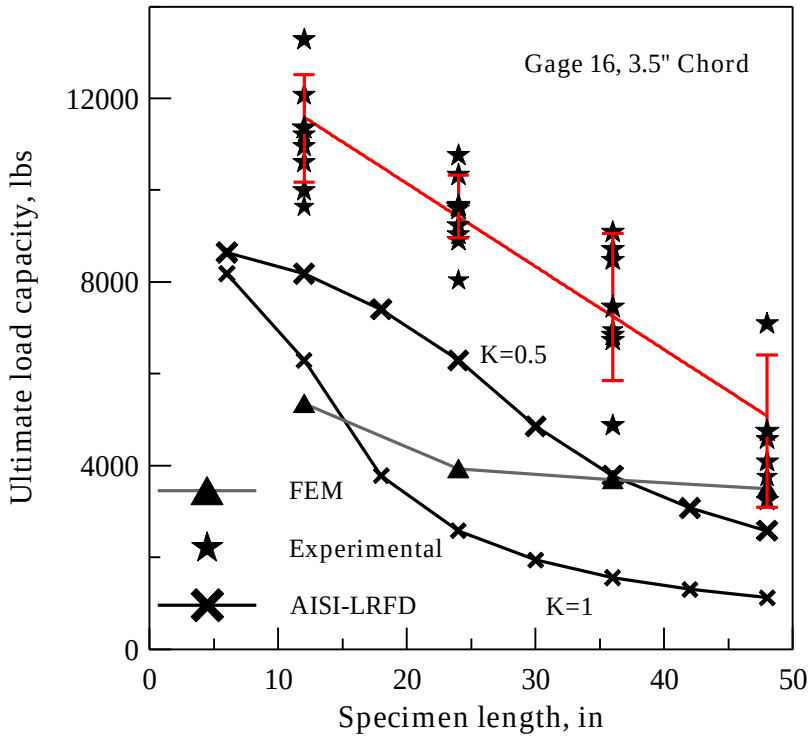

The values obtained from the laboratory test for four-point bending are compared with the AISI-LRFD design code and finite element analysis Table 2.

Table 2 Comparison of Results for the Four-Point Bending Test

	Positive Moment Capacity (lb-ft)					
	3.5 CHORD			2.5 CHORD		
Source	20 GA	18 GA	16 GA	20 GA	18 GA	16 GA
AISI-LRFD	81	122	209	80	120	204
FEA	159	276	487	205	320	512
Exp. Mean	430	739	1027	382	668	860
	Negative Moment Capacity (lb-ft)					
	3.5 CHORD			2.5 CHORD		
Source	20 GA	18 GA	16 GA	20 GA	18 GA	16 GA
AISI-LRFD	237	320	497	250	338	529
FEA	304	465	764	308	489	809
Exp. Mean	602	1047	1576	483	822	1212

Discussion of the Results on the Member Strengths

The following observations are relevant when comparing the results of the three different approaches.

(1) The experimental values are higher than either the AISI or the FEM values for all but two specimen types (they are however, within 2% and 10%). The experimental values reflect the peak value from the load-displacement curve. The post-peak strength is quite significant providing additional reserve stiffness and strength in the case of a design of a structure with redundancies. For systems with sufficient redundancy, the reserve strength may improve the factor of safety against overall failure. This behavior is not directly considered in a linear elastic based design.

(2) The deflection and deformation at peak load obtained from the experimental approach is significantly higher than the values obtained from the equivalent elastic approach. This is due to pre-peak nonlinearities observed in the experimental data as shown in Figure 2.

(3) The FEA values are larger than the AISI values for 19 out of the 24 cases for the Axial Compression Tests and for all the cases for the Four-Point Bending Tests. In cases where the FEA values are smaller than the AISI values, only one sample was more than 6% lower than the corresponding AISI value.

(4) The finite element based linearized buckling analysis is closer to the experimental values for cases with longer column lengths where the column follows an Euler buckling behavior. This may be attributed to the mesh refinement issues in capturing the local buckling modes.

(5) The use of the AISI-LRFD design code values provides conservative design values for the section sizes and lengths used in the present study. Based on this observation, AISI-LRFD Code guidelines were used in the subsequent sections for the truss design.

3.0 Optimal Design of Truss for Full Scale Testing

Several methodologies exist for optimal design of discrete structures such as trusses and frames. The methodology used in the present design of the roof truss is based on simultaneous sizing, shape, and topology design using genetic algorithm (GA) as the optimizer as discussed in Wright et.al [1995] and Chen and Rajan [1998]. The LRFD strength requirements for each member type were calculated based on the AISI specifications as a function of the unbraced length of the section. This ultimate strength versus section length curve was subjected to piecewise linear approximations describing the strength envelope curve. After a single finite element analysis was conducted, the forces in the member and its length were compared to the strength envelope data and the distance form the envelope curve were calculated. If the point corresponding to the member forces and length fell inside the curve, no penalty was assessed. To achieve an optimum design, the number of elements, and the cost of members must be minimized as well. The roof truss design problem is formulated as follows. The objective function is defined as the cost of the truss given as

$$f(\mathbf{x}) = \sum_{j=1}^{ne} c_j L_j + \sum_{k=1}^{nj} d_k + \sum_{l=1}^{nc} e \qquad (1)$$

where *ne* is the number of elements, *nj* is the number of joints, *nc* is the number of cuts made to obtain the truss members, L_j is the length of the element j, c_j is the cost per unit length, d_k is the cost of the connection (a function of the number of screws needed to construct the connection), and e is the cost of making a cut in a cold-rolled specimen so as to obtain a specified length member. The first term captures the material cost whereas the second and the third terms account for the labor cost.

The general steps followed in the design procedure are as follows.

(1) The design process is initiated by specifying the geometrical and loading parameters. These include the span, height of the King Post (or, the pitch of the roof), the dead and live loads acting on the top and bottom chords, heel heights and support conditions, the overhangs, and the truss spacing. Finally, the different types of cross-sections to consider for the members are specified.
(2) The truss structure is defined by the specification of the panel points, the maximum unbraced length of a bottom chord member or top chord members. Once the panel points are identified, the elements and nodes of the model are defined by connection of all the nodes to adjacent nodes. This creates what is popularly known as the ground structure (Fig. 5(a)).
(3) With the truss completely defined in terms of the topology (all the members with their cross-sectional properties and the member end nodal coordinates known), a materially linear, small displacement, small strain finite element analysis is carried out. The structure is assumed to be a planar frame with **rigid** connections. Second-order effects are neglected.
(4) Design checks based on the AISI code are carried out on the finite element results.
(5) The cost and design check data are then passed to the GA. The GA attempts to remove the elements that are inefficient (have a low stress magnitude) while the required elements that have their stress level exceeding the allowable stress are penalized by increasing their size and/or repositioning them. Step three is repeated again for the newly updated shape and geometry.
(6) At the end of the design process, one would obtain the cross-sections for the top and bottom chord, heels, King Post and the webs. The number of web sections and their location (in terms of the coordinates of the web members) are also determined.

Truss Design (for full-scale testing): The specific design problem is to design a roof truss with a span of 20’ and center-to-center spacing (between adjacent trusses) of 2’. The service design loading on the truss includes a live load of 16 psf and dead load of 24 psf acting on the top chord. The initial guess (or, also called ground structure) and the final design that was obtai-ned from the optimal design process are shown in Figs. 6(a)-(b). The truss contains a pin support at the bottom left (heel) and a roller support at the bottom right (heel). The dead plus live load (applied to the entire top chord as a uniformly distributed load) and the self-weight are converted to equivalent joint loads for the purposes of structural analysis. Cost figures supplied by the manufacturer were used in computing the labor and material costs. In the lowest cost truss, the top chords were 2.5” 16 GA sections, the bottom chords were 2.5” 18 GA sections, and the webs, King Post and the heels were 15” 18GA square tubes. The total weight of the truss was 74 lbs, the material cost was $38.65, the labor cost was $12.06 yielding a total cost of $51.71.

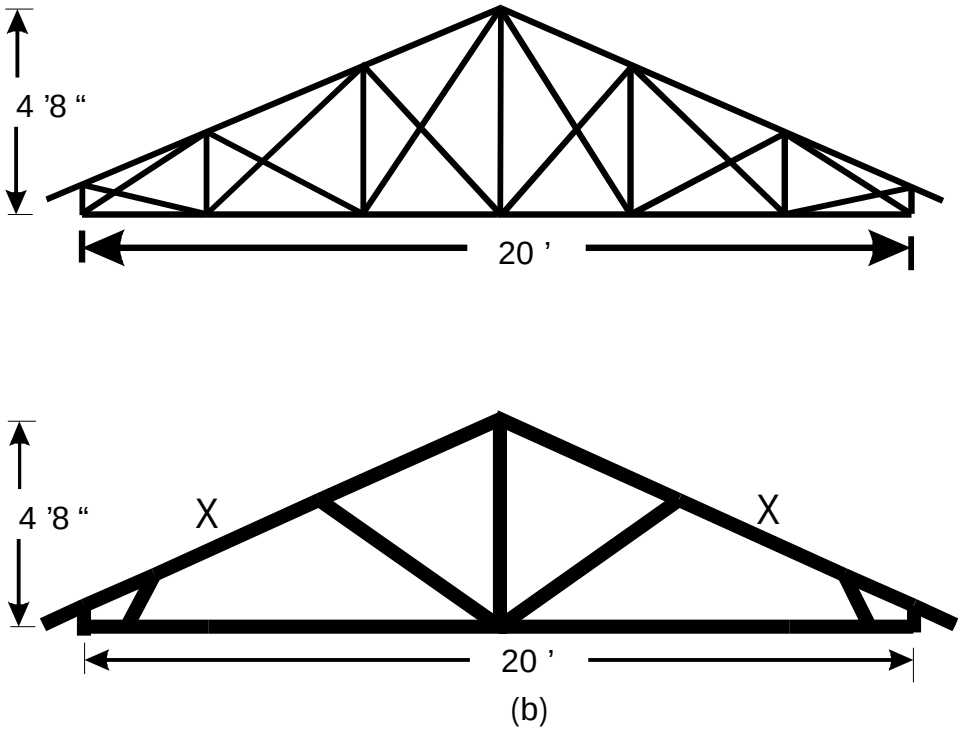

Fig. 6 (a) Initial guess and (b) the lowest cost truss obtained from the optimal design process

In the study presented the most critical sections are in the top left and right chord, and marked with an ‘**x**’ (Fig. 6(b)). In other words, the combined axial and bending effects in the top chord govern the performance of the truss.

4.0 Full Scale Testing

To prevent the truss from side sway buckling, a three-truss system was assembled with trusses placed @ 2' apart. They were joined continuously at the top chord using 0.5" thick plywood sheathing. Hat channels were used at 5’ spacing to connect the bottom chords of the trusses as well. Dead load was applied in incremental stages over the length of the top chord members by means of 50 lbs sandbags weighed individually and placed sequentially. In between each loading sequence, the response of the truss in terms of the applied load, the measured loads, the deflections, and strains in the members were recorded. Figs. 7(a)-(d) shows the different aspects of the full-scale test.

4.1 Test Details and Results

The instrumentation details as shown in Figs. 8(a)-(b) represent the front and side view of the test assembly. Due to the nature of loading shown in Fig. 6, only the middle truss is tested to failure by placing an equivalent dead load on the tributary roof area. The locations of the six load cells and three deflection dial gauges are shown In Fig. 8(a). The center truss spans the load cells labeled W2-E2 and the dial gauges labeled W, C and E.

Fig. 7(a) First stage of loading

Fig. 7(b) Stage 12 of loading

Fig. 7(c) Connections details at the top of the King Post

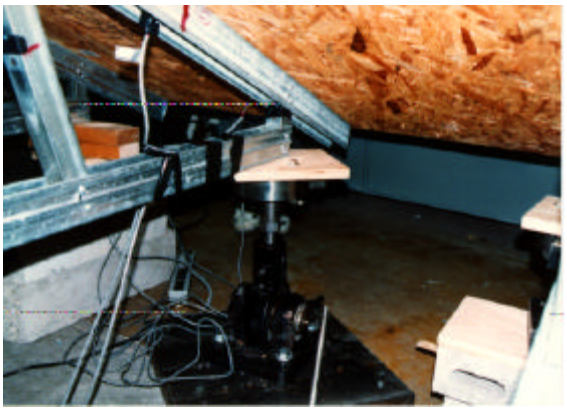

Fig. 7(d) Load cell labeled E1

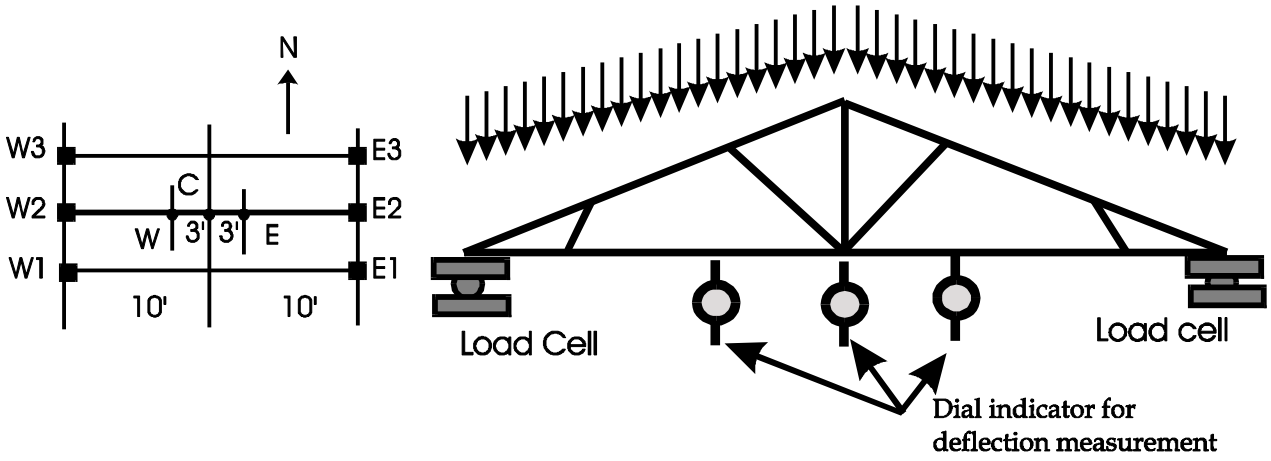

Fig. 8(a) Schematics of the instrumentation of the truss, load cells, and dial gauges

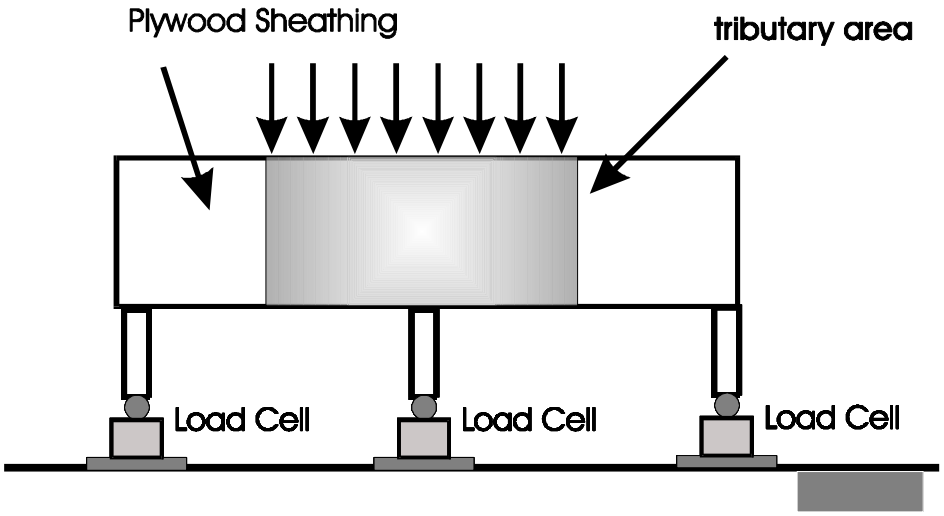

Fig. 8(b) Side view of the three truss assembly system

The truss loading was continued until a satisfactory level of factor of safety with respect to the design loads was achieved without any visual signs of failure in a member or at a joint. The deflection of the truss was recorded at three nodal points on the bottom chord using dial gages with a resolution of 0.001" and a range of 1" throughout the loading history. Fig. 9 represents the total load applied vs. the deflection response of the truss. As shown in the figure, the deflection of the bottom chord member is quite uniform throughout the length of the member for a major portion of the load applied. An initial linear response is seen until about 1600 lbs. The slopes of the curves change at this point and the second nearly linear response is observed until about 2500 lbs. Beyond that point, the response is nonlinear.

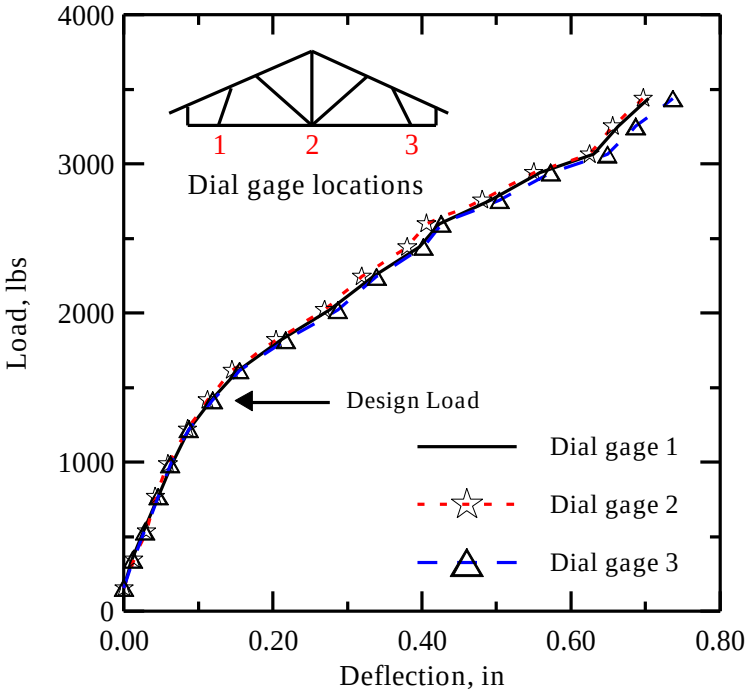

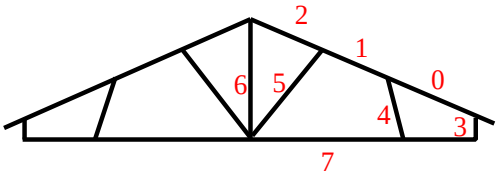

Fig. 9. Member strain versus total load for select members in the center truss

Fig. 10 Bottom chord deflections of the center truss versus total load applied on the center truss

The axial strains of several truss members were measured using resistance type strain gages that were placed at the center of the member. A total of 7 members were monitored throughout the test duration. The strain gage data were collected using a data acquisition system. Fig. 10 represents the axial strain in six members. It should be noted that the strain in these members remains relatively low as the truss is loaded.

At the time of termination of the test, there were no visual member or joint failures observed in the center truss. The combined load cell readings for the center truss was 3282 lbs. The design load was based on a total load of 1840 lbs. Based on the ratio of applied load to design load, the factor of safety for the truss used in the full-scale test is ***at least 1.8***. A comparison of the center truss load cell readings (W2 versus E2), shows that the load distribution is fairly even on both sides of the truss. The maximum level of deviation of load distribution was 10% at Stage 14. A comparison of the load cell readings for the outer trusses (W1, W3, E1 and E3) shows that the load distribution is fairly even to the outer trusses with a maximum difference of about 6% at Stage 16. Hence, load calculations based on the tributary areas are deemed to be adequate. There was a difference of 1% between the applied and measured forces on the truss.

Conclusions

A comprehensive system has been developed to design residential steel roof truss systems. The AISI-LRFD design code is used in the design process. The major AISI design curves that are applicable have been checked using experiment values as well as using finite element simulations. A GA-based design methodology has been developed that uses minimal input to automatically size, shape and configure the truss. The analysis and design processes are tested using a full-scale test of a 20’ span, flat-bottom truss.

Acknowledgments

The research sponsorship of Allied American Inc., Phoenix, AZ is greatly appreciated. Special thanks to Allied American personnel - Messrs. Robert Dixson, Matt Watson, Mike Meek, Dan Dry and Paul Shumway, for their contributions during the different stages of the research. Special mention should also be made of graduate students Joanne Situ, Dmitri Wright, Garrett Haupt, and Raj Vodela for their invaluable assistance in generating the design curves and conducting the full-scale testing.

References

American Institute of Steel Construction (1986) *Load and resistance factor design specification for structural steel building*.

American Iron and Steel Institute (1986), *AISI LRFD Cold-Formed Steel Design Manual, Part 1: Specification for Cold-Formed Steel Structural Members.*

ANSYS, Inc. (1997), ANSYS Theoretical Manual.

Chen, S-Y. and Rajan, S.D. (1998), Improving the efficiency of Genetic Algorithms for frame designs, *Engineering Optimization*, **30**, 281-307.

HKS, Inc. (1995), ABAQUS Theoretical Manual.

Hsiao, L-E, Yu, W-W and Galambos, V. (1990), AISI LRFD method for cold-formed steel structural members, *ASCE J of Structural Engineering*, **116**, 500-517.

Mobasher, B. and Situ, J. (1996), ICBO Test Report of the American Studco, Inc., Residential Roof Truss Chord Components, *Report No. CEE-AS-95-1*, Dept. of Civil Engineering, Arizona State University.

Rajan, S. D. (1995), Sizing, shape and topology design optimization of trusses using a genetic algorithm, *ASCE J Structural Engineering*, **121-10**, 1480-1487.

Salmon, C. and Johnson, J. (1990), *Steel Structures: Design and Behavior*. Harper Collins Publishers, New York.

Weng, C.C. and Pekoz, T. (1990), Compression tests of cold-formed steel columns, *ASCE J of Structural Engineering*, **116**, 1230-1246.

Wright, D., Situ, J., Mobasher, B. and Rajan, S.D. (1995), Development and implementation of an automated design system for steel roof trusses, *Proc. Research Transformed Into Practice: Implementation of NSF Research*, Eds. Colville and Amde, ASCE Press, Washington, D.C., 245-256.